Relative Coronal Abundances Derived From X-Ray Observations III: The Effe of Cascades on the Relative Intensity of Fe XVII Line Fluxes, and a Revised Iron Abundance

by

A.B.C. Walker, Jr., H. R. Rugge, and Kay Weis

August 1974

National Aeronautics and Space Administration
Grant NGR 05-020-695

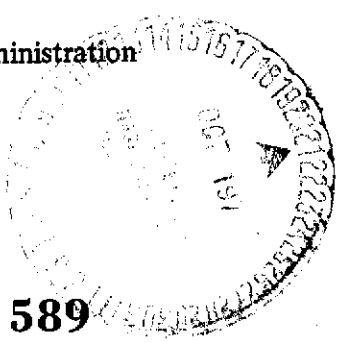

SUIPR Report No. 589

INSTITUTE FOR PLASMA RESEARCH
STANFORD UNIVERSITY, STANFORD, CALIFORNIA

RELATIVE CORONAL ABUNDANCES DERIVED FROM X-RAY OBSERVATIONS III: THE EFFECT OF CASCADES ON THE RELATIVE INTENSITY OF Fe XVII LINE FLUXES, AND A REVISED IRON ABUNDANCE

By

A.B.C. Walker, Jr.*, H.R. Rugge†, and Kay Weiss†

National Aeronautics and Space Administration
Grant NGR 05-020-695

SUIPR Report No. 589

August 1974

Institute for Plasma Research
Stanford University
Stanford, California

*Also Department of Applied Physics

†Space Physics Laboratory
The Aerospace Corporation
Los Angeles, California

ABSTRACT

Permitted lines in the optically thin coronal X-ray spectrum can be analyzed to find the distribution of coronal material as a function of temperature without special assumptions concerning coronal conditions, provided the relevant atomic rate constants are known. The helium-like and hydrogen-like resonance lines of N, O, Ne, Na, Mg, Al, Si, S, and Ar which dominate the quiet coronal spectrum below 25A have been observed from the U. S. Air Force satellites OV1-10 and OV1-17, and these observations have been used to construct coronal models and to determine the relative abundances of these elements. The theoretical atomic rate constants are relatively well known for these simple ions; and the coronal excitation condition, which assumes that excited states are populated by collisional excitation from the ground state, should be well satisfied for resonance lines of these ions. Lines of Fe XVII are also prominent in the coronal spectrum below 25A, and the intensity in the lines of the 2p-3d transitions near 15A has been used in conjunction with these coronal models, and with the assumption of coronal excitation, to determine the Fe abundance. There are 8 lines of Fe XVII observed from the $2p^5 3s$, $2p^5 3d$ and $2s2p^6 3d$ configurations in the coronal spectrum between 13 and 18A. Many of the upper levels are populated by cascade, so that the assumption of coronal excitation is not a valid one for most of these lines. Recent theoretical work on the spectrum of Fe XVII has taken account of the statistical equilibrium of the first 36 excited states in computing the intensity of the observed lines. Although the theoretical atomic rate constants of Fe XVII (especially the collisional excitation rates) cannot be as accurately calculated

as those of the simpler ions, the relative intensities of the 2p-3d Fe XVII lines observed in the corona are now in good agreement with theoretical predictions. The measured flux in the lines from the $2s^2 2p^5 3s$ levels, which are populated in part by cascade from the $2p^6 3\ell$ (ℓ = 1, 2, 3) levels, have been used to obtain the excitation rate coefficients for the $2s2p^6 3\ell\ ^3L$ levels, since the theoretical rate coefficients for these excitations are less accurately known than those for the 2p-3ℓ transitions. Using this more complete theoretical model, and higher resolution observations which allow a number of line blends to be resolved, we have revised our earlier calculation of the coronal abundance of Fe. We find an iron abundance relative to hydrogen of 26×10^{-6}, which is in excellent agreement with the photospheric iron abundance.

Subject Headings: abundances, solar-corona, solar-coronal lines-line identifications-X-rays, solar spectra-atomic processes.

1. Introduction

The pioneering work of Pottasch (1967 and the references cited therein) in analyzing EUV and soft X-ray spectra provided a detailed temperature structure for the quiet corona, and a technique to determine relative coronal abundances. Pottasch was able to include lines from a sufficient number of ionization stages of iron and of silicon (and consequently a broad temperature range for each element) to define a temperature structure for each element. The results of this analysis forced an increase of an order of magnitude in the coronal abundance ratio A_{Fe}/A_{Si} compared to the then currently accepted photospheric value. More recently, the relative abundance of iron in the solar wind has been measured directly (Bame, et al., 1970; Holtzer and Axford, 1970; Lange and Scheib, 1970). These results strongly support the revised iron abundances.

The redetermination of Fe I and Fe II oscillator strengths has led to the revision of the photospheric iron abundance (Gartz et al., 1969a) so that it is consistent with coronal determinations of the Fe/Si ratio (Jordan and Pottasch, 1968) and with results from meteorites (Gartz et al., 1969b) and the solar wind (Bame et al., 1970). Withbroe (1971) and Pagel (1974) have recently reviewed solar abundance determinations by a number of techniques, and in particular the studies of the abundance of iron using permitted EUV lines, which are excited primarily in the transition region.

In the present paper we study the abundance of iron in the hottest stable coronal configurations, the coronal condensations.

In two previous papers (Walker, Rugge, and Weiss, 1974a, b, hereafter referred to as papers I and II) we have used observations of lines of the helium-and hydrogen-like ions of nitrogen, oxygen, neon, sodium, magnesium, aluminum, silicon, sulphur, and argon, which are prominent in the spectrum of the quiet corona between 4 and 25A, to construct a coronal model, and to determine the relative abundance of these elements. The atomic rate constants required for the analysis are relatively well known for these simple ions [Walker (1972), Gabriel and Jordan (1972)], and the assumption of coronal excitation conditions (i.e., excited states are populated entirely by collisional excitation from the ground state) should not result in a significant error.

The lines of the neon-like ion Fe XVII are also observed in the spectrum of the quiet corona, and we have used the fluxes in these lines, and the model based on the hydrogenic and helium-like lines fluxes, to compute the relative coronal abundance of iron (paper II). However, the excited configurations of neon-like ions are complex, and a number of parent levels of strong lines are populated chiefly by cascade from higher levels. In the present paper we reexamine the coronal abundance of iron, using an improved theoretical model of the excitation of Fe XVII lines which includes the effects of cascades among 36 levels. We also use higher resolution spectral observations, which allow a number of lines which were blended with the Fe XVII lines in the spectra used in paper II to be resolved in the present analysis. We also discuss the agreement between the theoretical model of the excitation of the Fe XVII spectrum, and the observed coronal line fluxes, and derive values for the excitation rate coefficients from the ground level to the $2s2p^6 3(s, p, d)$ levels. The presently available theoretical excitation rate coefficients for these transitions are less reliable than those for the 2p-3(s, p, d) transitions.

2. Observations

In paper II we used the spectra obtained with the KAP crystal spectrometer on the OV1-10 satellite to determine the flux in the Fe XVII lines used for the abundance analysis. We believe the calibration of the OV1-10 spectra to be highly reliable; however, the resolution of the OV1-10 spectra is not sufficient to clearly resolve a number of the Fe XVII multiplets, or to resolve the question of the importance of possible line blends which might affect the accuracy of the observed line fluxes. In Figures 1 and 2 we show the Fe XVII lines observed in the higher resolution spectra obtained with the KAP crystal spectrometer on the OV1-17 satellite. The full spectra for this time period are shown in the paper by Walker and Rugge (1970). The spectra shown in Figures 1 and 2 were obtained at the same time as the EDDT spectra between 3.5 and 8.5 A which were analyzed in detail in paper I. The iron lines observed in the spectra of Figures 1 and 2, and in the spectra analyzed in paper II are listed in Table 1. The fluxes given in Table 1 have been corrected for line blends, as described below.

The calibration of the OV1-10 spectrometer was discussed in paper II. It was necessary to renormalize the calibration of the OV1-17 KAP spectrometer, since the inflight calibration data indicated a decrease in detector efficiency by a factor of 2 at a wavelength of $\sim$ 2A. Unfortunately it was not possible to provide an inflight calibration system at wavelengths within the range of the KAP spectrometer itself. We used the model constructed with the OV1-17 EDDT crystal spectrometer observations in paper I to calculate the Ne IX and O VIII resonance line fluxes, and determined a corrected KAP spectrometer calibration curve by comparing these calculated fluxes with the observed line intensities.

The strongest lines of Fe XVII are observed from the $2s^2 2p^5 3d$ and $2s^2 2p^5 3s$ configurations, with the two groups of multiplets being roughly equal in intensity. Pottasch (1966) pointed out that the small excitation cross-section for the $2s^2 2p^5 3s$ configuration was inconsistent with the assumption that this state is populated by direct excitation from the ground state; and he suggested that cascade from $2s^2 2p^5 3p$ was the main mode of populating the $2s^2 2p^5 3s$ configuration. Calculations by Bely and Bely (1967) confirmed the importance of excitation to $2s^2 2p^5 3p$; however, they did not consider the problem of the relative intensities of all of the observable lines in detail. Beigman and Urnov (1969) used cross-sections calculated in L-S coupling to calculate the relative intensities of the $2s^2 2p^5 3s$ multiplet group and of the individual lines of the $2s^2 2p^5 3d$ multiplet. Their results were in general agreement with observation. They also pointed out that the $2s^2 2p^5 3p$ level was itself populated to a considerable degree by cascade from the $2s2p^6 3p$ levels. Loulergue and Nussbaumer (1973) have recently calculated the relative intensities of each of the lines observed in the corona from the $2s^2 2p^5 3d$, $2s2p^6 3p$ configurations including cascades among 36 levels. In the present paper we compare these calculated line intensities and intensities calculated with a revised set of collisional excitation rates, with observations of the coronal spectrum made from the OV1-10 and OV1-17 satellites. The higher resolution OV1-17 observations, which have not been reported in detail previously, are of particular interest because they allow the intensities of the $^1S_0 - {}^3P_1$ (17.051Å) and forbidden $^1S_0 - {}^3P_2$ (17.10Å) transitions of the $2s^2 2p^5 3s$ configuration to be determined separately.

The identification of the Fe XVII lines is discussed by Parkinson (1973), who has observed these lines in a high resolution spectrum obtained with a rocket-borne spectrometer. The $2p^6\ ^1S_0 - 2p^5 3s\ ^3P_2$ line at 17.10 Å, which is clearly resolved from the $^1S_0 - ^3P_1$ line in the spectrum of Figure 2 and in the spectrum published by Parkinson, is of interest since it illustrates the importance of forbidden (in this case quadrupole) transitions in the low density corona. The higher resolution OV1-17 spectra allow us to resolve a number of lines which were blended with the Fe XVII 2p-3d multiplet in the OV1-10 spectra. In Table 2, we list the lines observed near the 2p-3d and 2p-3s multiplets in the spectra shown in figures 1 and 2. Parkinson has observed unidentified lines at $\sim$ 15.06 (this line is only partially resolved from the Fe XVII resonance line at 15.012Å), 15.10, 15.15, 15.21, 15.35, 15.43-15.53, 15.56, and 15.66Å near the 2p-3d multiplet, and lines at 16.83, 17.12, and 17.15Å, near the 2p-3s multiplet. The wavelengths of the weak lines observed in our spectra and by Parkinson are in reasonably good agreement. Parkinson suggests that these lines may be satellite lines due to transitions of the form $2p^6nl - 2p^5 3d(s)nd$ ($n \geq 3$) in Fe XVI. We assess the potential importance of line blends due to these satellite lines in the next section.

In Table 2, we have compiled a list of lines which could be blended with the Fe XVII lines, using the compilation of Kelly and Palumbo (1973), and the recent work on the fluorine (Fe XVIII) and oxygen (Fe XIX) isoelectronic sequences by Swartz et al (1971), Neupert et al (1973), Feldman et al (1973), Fawcett et al (1974), and Doschek et al (1974). The most serious potential blends are due to Fe XVIII and Fe XIX lines. Lines

of less abundant elements such as Cr will be too weak to cause significant blending. The blends which may be important are Fe XIX $2\ ^3P_2 - 3\ ^3S_1$ for the line at 15.012 Å. Fe XIX $2\ ^3P_0 - 3\ ^3P_1$ and Fe XVIII $2\ ^2P_{3/2} - 3\ ^2S_{1/2}$ for the line at 15.261 Å, and Fe XIX $2\ ^1S_0 - 3\ ^3S_1$ for the line at 15.45 Å. Unfortunately, it is difficult to calculate the flux in 2p - 3s transitions in Fe XVIII, and Fe XIX accurately, since collision strengths are not available for these ions, and cascades from $2p^4 3p$ and $2p^3 3p$ levels are probably important in populating the $2p^3 3s$ levels. However we may assess the strength of a blended line if we can observe the flux in a line from the same upper level, and if we know the relevant oscillator strengths. In the case of Fe XVIII $3\ ^2S_{1/2}$, we observe the transition $2\ ^2P_{1/2} - 3\ ^2S_{1/2}$ at 15.49 Å. We may obtain the oscillator strengths by interpolation from the results of Cohen et al. (1968) who calculated the gf values for these transitions in Mn XVII and Co XIX. We find that the flux in the Fe XVIII $2\ ^2P_{3/2} - 3\ ^2S_{1/2}$ line at 15.258 Å is $\sim$ 25% of that in the weak $2\ ^2P_{1/2} - 3\ ^2S_{1/2}$ line at 15.491 Å. The correction to Fe XVII $2\ ^1S - 3\ ^3D$ is less than 2%. For the Fe XIX lines at 14.971 Å ($2\ ^3P_2 - 3\ ^3S_1$) and at 15.453 Å ($2\ ^1S_0 - 3\ ^1P_1$), we may use the comparable transitions at 15.173 Å ($2\ ^3P_1 - 2\ ^3S_1$) and at 15.341 Å ($2\ ^1D_2 - 3\ ^1P_1$) respectively. We observe no significant line at 15.173 Å, and so assume that the line at 14.971Å is weak. We do observe a line at 15.33Å. However, if we assume that the transition probabilities are proportional to the statistical weights, the $2\ ^1S - 3\ ^1P$ line at 15.452Å is too weak to cause significant blending. For the $2\ ^3P_0 - 3\ ^3P_1$ transition at 15.237Å, there is no comparable transition which can be resolved in our spectra; however, the weakness of other Fe XIX lines suggests that this blend is unimportant as well.

In paper II, we assumed, for the 4 January 1967 spectra, that all of the flux observed between 15.0 and 15.5 Å, with the exception of an appropriate correction for the X-ray continuum, was due to the 3 Fe XVII 2s-3d transitions. Using the higher resolution OV1-17 observations, we may now correct the OV1-10 observations for 4 January 1967 for the weak lines which are listed in Table 2. The corrected fluxes are given in Table 1. The correction is 26% for 15.012 Å, 12% for 15.261 Å, and 50% for 15.452 Å.

3. Formulation of the Line Flux Integral Equation

The intensity of the lines emitted from an optically thin medium such as the corona is given by the volume integral of an emission function $E_{ij}\,[\,T_e(x_\nu),\ n_e(x_\nu)]$ which is a function of the local temperature and density of the medium. The emission function E_{ij} may be expressed as (Paper I)

$$1) \qquad E_{ij} = \frac{hc}{\lambda} A^{r}_{ij} \left\{ n_{z,i}\ [\,T_e(x_\nu),\ n_e(x_\nu)] + \sum_{n'l' > n_c l_c} n_{z-1,i'}\ [\,T_e(x_\nu),\ n_e(x_\nu)] \right\}$$

where $n_{z,\,i}$ is the population of the excited level i in ionization stage z, and $n_{z-1,i'}$ is the population of the doubly excited state with the same configuration as i, but with an additional electron, with the quantum numbers n'l'; and the summation is carried out over those states for which n'l' is sufficiently large that the wavelength of the emitted photon in'l' → jn'l' is unresolvable from that for transition i → j. The singly excited levels are populated chiefly by collisional excitation, and the doubly excited levels are populated chiefly by dielectronic recombination. For those cases where n'l' is small, the resulting satellite lines may be resolved from the parent line and their flux must be calculated separately. The line flux resulting from the decay of doubly excited levels is generally only a few percent of the observed resonance line flux, and has not been included in most previous analyses.

The population of the excited states $n_{z,i}$ can be calculated from the equations of statistical equilibrium (see, for example, Gabriel and Jordon 1972).

In the case of Fe XVII, we must include the effects of cascades, by solving the equations

$$2) \quad \frac{dn_{z,i}}{dt} = n_e n_{z,g} \alpha^{ex}_{gi} + \sum_{k>i} n_{z,k} A^r_{ki} - n_{z,i} \sum_{k<i} A^r_{ik}$$

where $n_{z,g}$ is the population of the ground level, α^{ex}_{gi} is the excitation rate from the ground level into the excited level i, and A^r_{ik} is the radiative decay rate from state i to state k. If we order the states according to energy, i=1 referring to the lowest lying excited state, and i=N to the highest excited state, the emission function which results from collisional processes can be written in terms of the equilibrium solution to equation 2) as

$$E^{ex}_{ij}(T_e, n_e) = \frac{hc}{\lambda_{ij}} A^r_{ij} n_{zi}$$

$$3) \quad = \frac{hc}{\lambda_{ij}} A^r_{ij} n_e n_{z,g} \frac{\sum_{k=i}^{N} \alpha^{ex}_{gk} \left| \Gamma_m \delta_{mp} - A^r_{mp} \right|}{\prod_{k=i}^{N} \Gamma_k}$$

where m = i+1, ... N; p = i, . . . k-1, . . . , N(i.e., $p \neq k$) and $A^r_{mp} \equiv 0$ for $p \geq m$. We have defined the total radiative width of the state k, $\Gamma_k = \sum_{k}^{1} A^r_{kl}$. The symbol δ_{mp} refers to the Kronecker delta [$\delta_{mp} = 1$, m=p, $\delta_{mp} = 0$ $m \neq p$].

Loulergue and Nussbaumer (1973) have calculated the emission functions for the lines listed in Table 1, taking into account cascades from the first 36 excited levels. A level diagram showing the principal radiative decay paths for these levels is shown in Figure 3. The levels which decay to the ground state are shown in bold type in Figure 3.

From equation 3 it is obvious that the population of each excited state, and consequently the intensity of all transitions, is proportional to the electron density, n_e, to the ground state population of the ion, $n_{z,g}$, and to the weighted sum of a set of collisional excitation rates from the ground state, α^{ex}_{gk}. Therefore, as Loulergue and Nussbaumer point out, the relative intensity of the observed Fe XVII lines will not be sensitive to electron density, and will be only slightly dependent on electron temperature [owing to the slightly differing temperature dependence of the α^{ex}_{gk} whose major temperature dependence will go as $\exp(-hc/\lambda_{gk}kT)$].

The intensities calculated by Loulergue and Nussbaumer are compared with the relative fluxes observed on OV1-10 and OV1-17, and by Parkinson (1973) in Table 3.

In the next section, we discuss the problem of selecting the best set of atomic rate constants for the solution of equation 3, and present a calculation of the relative intensities of the Fe XVII lines based on somewhat different assumptions regarding the $2s^2 2p^6$-$2s\ 2p^6 3s$, 3p, and 3d excitation rate coefficients than those made by Loulergue and Nussbaumer.

In equation 1, we included the flux resulting from decay of the doubly excited states in the sodium-like ion Fe XVI. The statistical equili-

brium equation for these states must include dielectronic recombination and collisional excitation as mechanisms for the population of excited states,

$$\frac{dn_{z-1,i'}}{dt} = n_e n_{z-1,g}\,\alpha^{ex}_{gi'} + n_e n_{z,g}\,\bar{\alpha}^{di}_{gi'} + \sum_{k'>i'} n_{z-1,k'}\,A^{r}_{k'i'} \qquad 4)$$

$$- n_{z-1,i'}\left[\sum_{k'<i'} A^{r}_{i'k'} + \sum_{j} A^{a}_{i'\,j\epsilon}\right] ,$$

$\bar{\alpha}^{di}_{gi'}$ is the total rate for the capture of an electron into the doubly excited state i', $A^{a}_{i'\,j\epsilon}$ is the rate for the inverse process in which a doubly excited state autoionizes emitting an electron of energy ϵ, and the other symbols have the same meaning as before. For lithium-like and helium-like ions collisional excitation of doubly excited states and cascades from other doubly excited states are negligible, and we may write the population of doubly excited states quite simply (Gabriel, 1972). However, in the case of sodium-like ions cascades from doubly excited states such as $2s2p^6 3s3p$ to $2s^2 2p^5 3s3p$ may well be important; and the Fe XVI ion has an appreciable population at sufficiently high temperatures that inner shell excitations such as $2s^2 2p^6 3s \rightarrow 2s^2 2p^5 3snl$ will be quite important [Goldberg et al. (1965), Bely (1967)].

However, if we use spectra of sufficiently high resolution so that transitions resulting from levels with n = 3 can be resolved, inner shell excitations can then contribute only to the flux in the Fe XVII 2p - 3s lines [Resolvable satellite lines to these lines have been reported previously by Rugge and Walker (1968) and by Parkinson (1973)]. Unresolvable satellites to the 2p - 3d resonance line (^1S - ^1P) will be due entirely to dielectronic recombination, and the term containing $\alpha^{ex}_{gi'}$, in equation 4 may be neglected for this transition. Cascades of the type $2s^2 2p^5\ n'(p, f)\ n\ell \rightarrow 2s^2 2p^5 3d\ n\ell$, and $2s2p^6 3d\ n\ell \rightarrow 2s^2 p^5\ 3d\ n\ell$ can contribute to the emission of unresolvable

satellites to the 2p-3d lines. However, since dielectronic recombination rates are proportional to oscillator strengths, rates for the 2s-2p transition (where $\Delta n = 0$) will be small, while the small intensity of the singly excited 2p - 4d transitions [$\sim 10\%$ of the 2p - 3d resonance line (from Table 4)] suggests that these higher excitations will not be significant. The population of doubly excited levels due to cascades should, therefore, be small. The population of the doubly excited levels, (z-1, i') may then be expressed as

$$n_{z-1,i'} = n_e n_{Z'g} \bar{\alpha}^{di}_{gi'} \Big/ (\Gamma^r_{i'} + \Gamma^a_{i'}) = n_e n_{Z-1,g} \alpha^{di}_{gi'} \Big/ A^r_{i'g}$$

where (Shore, 1969)

$$\bar{\alpha}^{di}_{gi'} = \frac{1}{2} \left[\frac{2\pi\hbar^2}{mkT_e}\right]^{3/2} \frac{g'_i}{g_g} A^a_{gi'} \exp(-hc/\lambda_{gi'} kT_e) .$$

The g's are statistical weights. Burgess (1965) and Shore (1969) have discussed the sum of the dielectronic recombination rates, $\alpha^{di}_{gi'}$, for the states i' (i.e., in'ℓ') over large values of n'ℓ' . This sum is the quantity required in the evaluation of equation 1. Tucker and Koren (1971) have developed a simple expression which approximates Shore's results. Tucker and Koren find that the ratio of flux due to dielectronic recombinations, and that due to collisional excitation may be written

$$E^{di}/E^{ex} \approx 40(Z+1)^3 / T_e .$$

For the Fe XVII 2p-3d resonance line this results in a 4% enhancement at $\sim 5 \times 10^6$ °K . We shall assume that dielectronic contributions to the non-resonance transitions (^1S-^3P) and (^1S-^3D) are negligible.

Using the formalism developed in paper I, we may write the flux in the Fe XVII 2p-3d multiplet, which was used in paper II to derive the iron abundance, as

$$F_{2p\text{-}3d} = \sum_{ij} \epsilon(\lambda_{ij})\, a_H\, A_{Fe} \iint dSN_e \int dT_e\, n_e(T_e)\phi(T_e) \times$$

5)

$$a_{Fe\ XVII}(T_e) \times [J^{ex}{}_{ij}(T_e) + J^{di}{}_{ij}(T_e)]$$

where we may write the excitation functions $J^{ex}{}_{ij}$ as

$$6) \qquad J^{ex}{}_{ij} = \frac{hc}{\lambda_{ij}}\, A^r{}_{ij}\, \frac{\sum_{k=i}^{N} \alpha^{ex}{}_{gk} \left| \Gamma_m \delta_{mp} - A^r{}_{mp} \right|}{\prod_{k=i}^{N} \Gamma^r_k} ,$$

and the function $J^{di}{}_{ij}$ as

$$J^{di}{}_{ij} = \frac{hc}{\lambda_{ij}}\, \alpha^{ex}{}_{ij}\, \frac{1.95 \times 10^{-5}}{T_e}\, \frac{A^r_{ij}}{\Gamma^r_i}$$

The sum over ij extends over the $^1S_0$ - $^1P_1$, $^1S_1$ - $^3D_1$, and $^1S_0$ - $^3P_1$ transitions for J^{ex}, and over $^1S_0$ - $^1P_1$, only for J^{di}. The quantity $N_e n_e(T_e)\, \phi\, (T_e)$ is the emission measure of the corona as a function of temperature, $a_{Fe\ XVII}(T_e)$ is the fractional population of iron ions in the Fe XVII state, A_{Fe} the abundance of iron, a_H the number of electrons per hydrogen ion, and $\epsilon(\lambda_{ij})$ the spectrometer efficiency function [$\epsilon(\lambda_{ij})$ also includes the geometrical factor $1/4\pi(A.U.)^2$]. The integral over the area unresolved by the spectrometer, S, is extended over the entire disk for the OV1-10 and OV1-17 observations.

4. Determination of Atomic Rate Constants

Loulergue (1971) has calculated the energies for all levels in Table 2, and the radiative decay rates for all electric dipole transitions. Garstang (1966, 1969) has calculated the decay rates for those levels which have magnetic dipole or quadrupole decays of importance. Bely and Bely (1967) have calculated collision strengths for excitations to the $2s^2 2p^5 3s$, $2s^2 2p^5 3p$, and $2s^2 2p^5 3d$ configurations in intermediate coupling, for those levels which have strong excitation cross-sections. For the excitations to the $2s2p^6 3s$, $2s2p^6 3p$, and $2s2p^6 3d$ singlet levels, Bely and Bely have extrapolated lithium-like cross-sections, viz.

$$Q(2s^2 2p^6 \rightarrow 2s2p^6 nl) = Q(2s^2 \rightarrow 2snl)$$

and

$$Q(2s^2 \longrightarrow 2snl) = 2Q(2s \longrightarrow nl) .$$

However, Bely and Bely do not calculate or estimate cross-sections for excitations to the $2s2p^6 3s$, $2s2p^6 3p$, or $2s2p^6 3d$ triplet levels. Beigman and Vainshtein (1968) do calculate cross-sections for both the $2s2p^6 3\ell$ singlet and triplet levels; however, they do not include configuration interaction in their calculations. According to Bely and Bely, configuration interaction will be important for these levels.

Flower (1971) has calculated excitation cross-sections in L-S coupling for a number of levels for which Bely and Bely do not present results. Loulergue and Nussbaumer have used the cross-sections of Bely and Bely where available, and the results of Flower for other levels. For the excitations to the $2s2p^6 3s$, $2s2p^6 3p$, and $2s2p^6 3d$ triplet levels, Loulergue and Nussbaumer assumed that the triplet cross-sections are equal to the singlet cross-sections multiplied by the ratio of statistical weights.

We have chosen to use the cross-sections for beryllium-like ions to obtain cross-sections for the $2s2p^6 3s$, and $2s2p^6 3d$ singlet excitations, using the relation

$$Q(2s^2 2p^6\ {}^1S \rightarrow 2s2p^6\ 3\ell\ {}^1L) = Q(2s^2\ {}^1S \rightarrow 2s3\ell\ {}^1L)$$

We have used the observed relative fluxes of the $2s^2 2p^6\ {}^1S - 2s2p^6 3p\ {}^1P$ and ${}^3P$ transitions to derive the collisional excitation rates into their respective upper levels. We believe this approach is justified because the upper levels of these lines are not appreciably populated by cascade, and should satisfy the coronal excitation condition, with the result that the line fluxes are directly proportional to the respective excitation coefficients and the branching ratios. Finally, we have used the relative fluxes in the $2s^2 2p^5 3s\ {}^1P$ and ${}^3P$ transitions to derive the collisional excitation rates into the $2s2p^6 3s\ {}^3S$ and $2s2p^6 3d\ {}^3D$ levels. Since the $2s^2 2p^5 3s$ levels are populated by cascade from a large number of levels, the values of the ${}^3S$ and ${}^3D$ cross-sections derived depends on the accuracy of the theoretical cross sections for these other levels, as well as on the accuracy of the experimental line intensity ratios.

Gabriel and Jordan (1972) have reviewed the published cross-section data for beryllium-like ions. Theoretical calculations for the cross-sections of interest have been carried out by Eissner (1972), and experimental measurements have been made by Johnson and Kunze (1971) and Tondello and McWhirter (1971). We have used the Ne VII excitation rates calculated by Eissner and extrapolated to higher Z using the Z dependence of the lithium-like $2s$-3ℓ excitations calculated by Bely (1966), to obtain values of Ω for Fe XVII. The collision strengths which we have adopted are

presented in Table 4. The calculated Fe XVII line intensities which we derive, using the collision strength given in Table 4 and the same set of radiative transition rates as Loulergue and Nussbaumer, are compared with the experimental results in Table 3. The ratios tabulated are calculated for 4.0×10^6 °K. We have chosen this temperature since it is the temperature of most efficient excitation for Fe XVII lines for the coronal temperature structure derived for 20 March 1969 in paper II. Both sets of theoretical calculations are in reasonably good agreement with the observations, and it is difficult to argue that the experimental data favors either set of calculated fluxes. In Table 5, we have tabulated the quantity $J^{ex}_{ij}(T_e) / [\alpha^{ex}_{gi}(hc/\lambda_{ij})(A^r_{ij}/\Gamma_i)]$, which is the ratio of line fluxes which would be calculated including cascades, to those which would be calculated without including cascades. The results in Table 3 include the effects of dielectronic recombination, while those in Table 5 do not.

5. Calculation of the Revised Iron Abundance

In paper II, we calculated the abundance of iron using equation 5, and the coronal emission measure model developed from an analysis of O VII, O VIII, Ne IX, Ne X, and Mg IX line fluxes. In the present paper we follow the same procedure, using the OVI-10 Fe XVII 2p-3d multiplet line fluxes, and the improved Fe XVII line excitation functions derived from section 4. We have also corrected the observed OV1-10 fluxes for the blending caused by the unidentified satellite lines observed in the higher resolution OV1-17 spectra, and listed in Table 2. As discussed in Section 2, this correction was accomplished by multiplying the OV1-10 fluxes by the ratio of the flux observed in the 2p-3d multiplet to the total line flux observed between 15 and 15.5A for the OV1-17 spectra. We believe this procedure is justified since the analysis carried out in papers I and II found that the coronal temperature structure derived from the two sets of observations were the same, so that the relative Fe XVII line intensities and Fe XVI satellite line intensities should be the same for both spectra. The corrected OV1-10 2p-3d multiplet fluxes are given in Table 1. Using the corrected flux, and using the improved Fe XVII line excitation functions, we find the revised iron abundance to be $A_{Fe} = 26 \times 10^{-6}$. This abundance assumes a silicon abundance normalized to $A_{Si} = 35 \times 10^{-6}$, as discussed in papers I and II. This revised iron abundance agrees more closely with the value of 25×10^{-6}, found in recent photospheric analyses [Withbroe (1971), Smith and Whaling (1973)], than the value of 40×10^{-6} which was found in paper II.

6. Summary

We have calculated the relative intensity of eight Fe XVII lines observed in the coronal spectrum between 13 and 18A, and find that these theoretical intensity ratios are in reasonably good agreement with observations. Using the improved line emission functions calculated from this analysis, we have used the Fe XVII $2p^6\ ^1S\text{-}2p^5 3d\ ^1P$, ^3D, and ^3P line fluxes, and a coronal model derived from the analysis of O VII, O VIII, Ne IX, Ne X, and Mg XI line fluxes to compute the abundance of iron in the corona. We find $A_{Fe} = 26 \times 10^{-6}$, which is in good agreement with the photospheric iron abundance [Smith and Whaling (1973)], and with the coronal iron abundance determined from the analysis of XUV fluxes (Dupree, 1971). The coronal abundances found in papers I and II, and in the present paper are summarized in Table 6, and compared with transition region and photospheric abundances.

We have also compared the results of papers I and II, and the present paper with the recent compilation by Cameron (1974) of solar system abundances in Table 6. In general, the agreement is good; however, there is a significant difference for the neon abundance. Cameron's neon abundance is obtained from cosmic ray observations. Since the neon lines used in our analysis were quite strong, and were excited near the mid-range of temperatures in our model (paper II) we believe our neon results to be quite reliable, and the difference may, therefore, be significant. In the case of the sulfur and argon abundances, the lines analyzed were near the high temperature end of our model (paper I), and are thought to be somewhat less reliable than the other abundances. Consequently, we do not regard

the difference between our results and Cameron's computation to be significant for these elements.

We should like to thank Drs. Loulergue and Nussbaumer for allowing us to see their results in advance of publication, and for several useful comments and suggestions during the course of our investigation. We would like to thank Dr. Loulergue for sending the results of some of her unpublished calculations, and Dr. Parkinson for communicating his results to us in advance of publication. We are grateful to Dr. Eissner for sending us the results of his theoretical calculations of beryllium-like excitation

We would also like to thank Dr. H. H. Hilton and Mrs. M. Wray for their help in the theoretical calculations, and Dr. D. Cartwright for a helpful discussion on the problems associated with extrapolating the beryllium-like cross-sections. We are grateful to Mrs. A. Keys and Mrs. J. Chafe for typing the manuscript. This work was supported in part by the National Aeronautics and Space Administration under Grant NGR 05-020-695.

Table 1

Fe XVII LINES OBSERVED IN THE CORONAL SPECTRUM

	j - j	WAVELENGTH (A)	Flux (10^{-5} ergs/cm^2-sec) 4 Jan 1967	20 Mar 1969
$2s^2\ 2p^5\ 3s\ ^3P - 2s^2\ 2p^6\ ^1S$	2 - 0	17.10	131	458
$3s\ ^3P - 2s^2\ 2p^6\ ^1S$	1 - 0	17.05		492
$3s\ ^1P - 2s^2\ 2p^6\ ^1S$	1 - 0	16.77	73	442
$3d\ ^3P - 2s^2\ 2p^6\ ^1S$	1 - 0	15.45	5 *	56
$3d\ ^3D - 2s^2\ 2p^6\ ^1S$	1 - 0	15.26	44 *	342
$3d\ ^1P - 2s^2\ 2p^6\ ^1S$	1 - 0	15.01	104 *	610
$2s\ 2p^6\ \ 3p\ ^3P - 2s^2\ 2p^6\ ^1S$	1 - 0	13.88	--	18
$3p\ ^1P - 2s^2\ 2p^6\ ^1S$	1 - 0	13.82	--	43
$2s^2\ 2p^5\ 4d\ ^3D - 2s^2\ 2p^6\ ^1S$	1 - 0	12.26	7.8 **	--
$4d\ ^1P - 2s^2\ 2p^6\ ^1S$	1 - 0	12.12	4.3	--

* These line fluxes have been corrected for blending due to the lines in Table 2.

** Parkinson (private communication) has resolved a number of lines which are blended with the Fe XVII $2\ ^1S - 4\ ^3D$ line in the OV1-10 spectra. The absolute flux given in this table should, therefore, be treated with caution.

TABLE 2

Lines Observed Near the Fe XVII 2p-3s and 2p-3d Transitions for the 20 March 1969 Spectra

Observed Wavelength (A)	Predicted Wavelength (A)	Ion	Transitions	j-j
17.10	17.10	Fe XVII	$2s^2 2p^6\ ^1S\text{-}2s^2 2p^5 3s\ ^3P$	0-2
	17.09	Cr XVI	$2s^2 2p^5\ ^2P\text{-}2s^2 2p^4 3d\ ^2D$	1/2-3/2
17.06	17.051	Fe XVII	$2s^2 2p^6\ ^1S\text{-}2s^2 2p^5 3s\ ^3P$	0-1
16.92				
16.90				
16.83				
16.77	16.775	Fe XVII	$2s^2 2p^6\ ^1S\text{-}2s^2 2p^5 3s\ ^1P$	0-1
. . . . .				
-	15.623	Fe XVIII	$2s^2 2p^5\ ^2P\text{-}2s^2 2p^4(^1D)3s^2D$	3/2-5/2
-	15.598	Fe XIX	$2s^2 2p^4\ ^1S\text{-}2s^2 2p^3 S\ ^3P$	0-1
-	15.567	Fe XVIII	$2s^2 2p^5\ ^2P\text{-}2s^2 2p^4 3s\ ^2D$	3/2-3/2
15.54				
15.51				
15.49	15.491	Fe XVIII	$2s^2 2p^5\ ^2P\text{-}2s^2 2p^4 3s\ ^2S$	1/2-1/2
15.45	15.452	Fe XVII	$2s^2 2p^6\ ^1S\text{-}2s^2 2p^5 3d\ ^3P$	0-1
	15.452	Fe XIX	$2s^2 2p^4\ ^1S\text{-}2s^2 2p^3 3s\ ^1P$	0-1
-	15.413	Fe XIX	$2s^2 2p^4\ ^1D\text{-}2s^2 2p^3 3s\ ^3P$	2-1
15.36	15.361*	Fe XIX	$2s^2 2p^4\ ^3P\text{-}2s^2 2p^3 3s\ ^3P$	0-1
15.33	15.341*	Fe XIX	$2s^2 2p^4\ ^1D\text{-}2s^2 2p^3 3s\ ^1P$	2-1
-	15.306	Fe XIX	$2s^2 2p^4\ ^1D\text{-}2s^2 2p^3 3s\ ^3P$	2-1
-	15.288	Fe XIX	$2s^2 2p^4\ ^3P\text{-}2s^2 2p^3 3s\ ^1P$	1-1

TABLE 2 (Continued)

Observed Wavelength (A)	Predicted Wavelength (A)	Ion	Transitions	j-j
	15.261	Fe XVII	$2s^2 2p^6\ {}^1S\text{-}2s^2 2p^5 3d\ {}^3D$	0-1
15.26	15.258	Fe XVIII	$2s^2 2p^5\ {}^2P\text{-}2s^2 2p^4({}^1S)3s\ {}^2S$	3/2-1/2
-	15.237	Fe XIX	$2s^2 2p^4\ {}^3P\text{-}2s^2 2p^3 3s\ {}^3P$	0-1
15.21				
15.19				
-	15.176	O VIII	$1s\ {}^2S - 2p^2 p$	1/2-3/2
-	15.173	Fe XIX	$2s^2 2p^4\ {}^3P\text{-}2s^2 2p^3 3s\ {}^3S$	1-1
-	15.158	Fe XIX	$2s^2 2p^4\ {}^1D\text{-}2s^2 2p^3 3s\ {}^1P$	2-1
15.13	15.132*	Fe XIX	$2s^2 2p^4\ {}^3P\text{-}2s^2 2p^3 3s\ {}^3S$	0-1
-	15.110	Fe XIX	$2s^2 2p^4\ {}^3P\text{-}2s^2 2p^3 3s\ {}^1P$	0-1
15.08	15.083*	Fe XIX	$2s^2 2p^4\ {}^3P\text{-}2s^2 2p^3 3s\ {}^1P$	2-1
-	15.069	Fe XIX	$2s^2 2p^4\ {}^3P\text{-}2s^2 2p^3 3s\ {}^3P$	2-2
15.01	15.012	Fe XVII	$2s^2 2p^6\ {}^1S\text{-}2s^2 2p^5 3d\ {}^1P$	0-1
	14.971	Fe XIX	$2s^2 2p^4\ {}^3P\text{-}2s^2 2p^3 3s\ {}^3S$	2-1
-	14.927	Fe XIX	$2s^2 2p^4\ {}^3P\text{-}2s^2 2p^3 3s\ {}^1P$	2-1

* These Fe XIX lines are coincident in wavelength with the observed lines; however, transitions in doubly excited states of Fe XVI may be partly responsible for the observed line flux.

Table 3

COMPARISON OF EXPERIMENTAL AND THEORETICAL LINE INTENSITIES

TRANSITION		THEORY			EXPERIMENT		
	(Å)	(1)	(1)'	(2)	4 Jan 1967(2)	20 Mar 1969(2)	30 Nov 1971(3)
3s - 2p	17.10	0.23	0.74	.59	1.25	0.75	0.64
3s - 2p	17.05	0.58	0.97	.91		0.80	0.82
3s - 2p	16.77	0.38	0.54	.51	0.70	0.72	0.58
3d - 2p	15.45	0.008	0.08	.09	0.05	0.09	0.11
3d - 2p	15.26	0.33	0.37	.37	0.43	0.56	0.50
3d - 2p	15.01	1.00	1.00	1.00	1.00	1.00	1.00
3p - 2s	13.88	0.002	.10	.03	--	0.03	0.04*
3p - 2s	13.82	0.15	.15	.07	--	0.07	0.07
4d - 2p	12.26	--	--	--	0.07	--	--
4d - 2p	12.12	--	--	--	0.04	--	--

(1) Loulergue and Nussbaumer (T=5.5x10^6) $\left[\Omega_{2s^2 2p^6\ {}^1S - 2s2p^6 3\ell\ {}^3L} \equiv 0\right]$

(1)' Loulergue and Nussbaumer (T=5.5x10^6)

(2) Walker, Rugge, and Weiss (T=4.0x10^6)

(3) Parkinson

* The ratios for Parkinson spectra are taken from Loulergue and Nussbaumer. Examination of Parkinson spectra by the present authors suggests .04 is closer to Parkinson's measured ratio than the value of .05 quoted by Loulergue and Nussbaumer.

Table 4

THRESHOLD COLLISION STRENGTHS FOR Fe XVII

Configuration	Level	Collision Strength ($\times 10^3$)		Ref.
$2s2p^6 3d$	$^1D_2$	65.2	(73)*	Bely & Bely
	$^3D_1$	--	(100)**	
	$^3D_2$	--		
	$^3D_3$	--		
$2s2p^6 3p$	$^1P_1$	22.4	(10.1)**	Bely & Bely
	$^3P_2$	--		
	$^3P_0$	--		
	$^3P_1$	--	(6.5)**	
$2s2p^6 3s$	^1S_o	32.4	(30.1)*	Bely & Bely
	$^3S_1$	--	(45)**	
$2s^2 2p^5 3d$	$^1P_1$	147		Bely & Bely
	$^1D_2$	2.9		Flower
	$^3F_3$	--		
	$^3F_2$	19.8		Flower
	$^3D_1$	47.3		Bely & Bely
	$^3D_3$	--		

* Collision strengths extrapolated from the Beryllium-like collision strengths calculated by Eissner.

** Collision strengths derived from observed coronal line ratios in this paper.

Table 4 (Cont.)

Configuration	Level	Collision Strength ($\times 10^3$)	Ref.
$2s^2 2p^6 3d$	$^3D_2$	--	
	$^3P_2$	17	Flower
	$^3F_4$	--	
	$^1F_3$	4.1	Flower
	$^3P_1$	1.2	Bely & Bely
	$^3P_0$	3.8	Flower
$2s^2 2p^5 3p$	$^1S_0$	64	Bely & Bely
	$^3P_2$	0.6	Bely & Bely
	$^3P_1$	4.7	Flower
	$^1P_1$	1.6	Flower
	$^3P_0$	3.4	Bely & Bely
	$^1D_2$	0.5	Bely & Bely
	$^3D_1$	11.6	Flower
	$^3D_3$	--	
	$^3D_2$	0.4	Bely & Bely
	$^3S_1$	4.7	Flower
$2s^2 2p^5 3s$	$^1P_1$	1.45	Bely & Bely
	$^3P_0$	--	
	$^3P_1$	1.67	Bely & Bely
	$^3P_2$	--	

TABLE 5

Calculated Ratios of Fe XVII Line Intensities
(Ratios are given in photons at 4×10^6 °K)

Line	Cascades Included	Cascades Not Included
17.10A	.62	0
17.05	.96	.017
16.77	.54	.013
15.45	.10	.014
15.26	.39	.33
15.01	1.05	1.00
13.88	.03	.03
13.82	.07	.07

TABLE 6

Comparison of Relative Abundances

Element	Abundance ($\times 10^6$)				
	Active Region	Transition Region		Photospheric	Solar System
	Walker, et al.	Withbroe	Dupree	Withbroe	Cameron
N	90	89	150	115	117
O	700	450	595	676	676
Ne	54	28	27	-	108
Na	1.7	2.3	1.9	1.7	1.9
Mg	30	35	30	35	33
Al	2.5	2.3	3.5	2.5	2.7
Si	35*	35*	35*	35	31.6
S	9	11	20	16	16
Ar	6	4.5	-	-	3.7
Fe	26	35	20	25†	26

† In a recent analysis, Smith and Whaling (1973) find a value of 25×10^{-6} for the iron abundance, in agreement with the earlier result of Withroe.

* The coronal abundance values have been normalized relative to the silicon abundance, which was assumed to be 35×10^{-6}.

REFERENCES

Bame, S. J., Asbridge, J. R., Hundhausen, A. J., and Montgomery, M. P., 1970, J. Geophys. Res. 75, 6360.

Bely, O., 1966 Ann. d' Astrophys. 29, 683; 1967 ibid 30, 953.

Bely, O., and Bely, F., 1967, Solar Phys. 2, 285.

Cameron, A. G. W. 1974, Space Sci. Rev. 15, 121.

Chapman, R. D. and Shadmi, Y., 1973, J. Opt. Soc. Am. 63, 1440

Cohen, L. Feldman, U. and Kastner, S. O., 1968, J. Opt. Soc. Am. 58, 331.

Doschek, G. A., Feldman, U., and Cohen, L. 1973, J. Opt. Soc. Am. 63, 1463

Dupree, A. K., 1972, Astrophys. J. 178, 527.

Eissner, W., 1972, Unpublished results quoted by Gabriel and Jordan (1972), and private communication.

Fawcett, B. C., Cowan, R. D. and Hayes, R. W. 1974, Ap. J. 187, 377.

Feldman, U., Doschek, G. A. Cowan, R. D., and Choen, L. 1973, J. Opt. Soc. Am. 63, 1445.

Flower, D. R., 1971, J. Phys. B 4, 697.

Gabriel, A. H., 1972, M.N.R.A.S. 160, 99.

Gabriel, A. H., and Jordan, Carole, 1972, Case Studies in Atomic Collision Physics II Ed: E. W. McDaniel and M. R. C. McDowell (North Holland Pub. Co., Amsterdam) p. 211.

Garstang, R. H., 1966, Publ. Astron. Soc. Pacific 78, 399.

Garstang, R. H., 1969, Publ. Astron. Soc. Pacific 81, 488.

Gartz, T., Holweger, H., Kock, M., Richter, J., Boschek, B., Holweger, H., and Unsold, A., 1969a, Nature, 222, 1254.

Gartz, T., Holweger, H., Kock, M., and Richter, J., 1969b, Astron. & Astrophys. 2, 446.

Goldberg, L., Dupree, A. K., and Allen, J. W., 1965, Ann. d' Astrophys. 28, 589.

Holtzer, T. E., and Axford, W. J., 1970, J. Geophys. Res. 75, 6354.

Johnson, W. D., and Kunze, H. J., 1971, Phys. Rev. A 4, 962.

Jordan, C., and Pottasch, S. R., 1968, Solar Phys. 4, 104.

Jordan, C., 1970, M.N.R.A.S. 149, 1.

Kelly, R. L., and Palumbo, L. J. 1973, Atomic and Ionic Emission Lines Below 2000 Angstroms, Hydrogen through Krypton, NRL Report 7699, U. S. Government Printing Office, Washington, D. C.

Lange, J., and Scherb, F., 1970, J. Geophys. Res. 75, 6350.

Loulergue, M., 1971, Astron. & Astrophys. 15, 216.

Loulergue, M., 1973, Private communication.

Loulergue, M., and Nussbaumer, H., 1973, Astron. & Astrophys. 24, 312.

Neupert, W. N., Swartz, M., and Kastner, S. O., 1973, Solar Phys. 31, 171.

Nussbaumer, H., 1969, M.N.R.A.S. 145, 141.

Pagel, B. E. J. 1974, Space Sci. Rev. 15, 1.

Parkinson, J. H., 1973, Astron. & Astrophys. 24, 215.

Pottasch, S. R., 1966, Bull., Astron. Inst. Neth. 18, 237.

Pottasch, S. R., 1967, Bull., Astron. Inst. Neth. 19, 113.

Rugge, H. R. and Walker, A. B. C., Jr., 1968, in [A. P. Mitra, L. G. Jacchia and W. S. Neuman (eds.)] Space Res. 8, North Holland Pub. Co. (Amsterdam) p. 439.

Shore, B., 1969 Astrophys. J. 158, 1205.

Smith, P. L. and Whaling, W., 1973, Astrophys. J. 183, 313.

Tondello, G., and McWhirter, R. W. P., 1971, J. Phys. B 4, 715.

Walker, A. B. C., Jr. 1972, Space Sci. Rev. 13, 672.

Walker, A. B. C., Jr., and Rugge, H. R., 1970, Astron. & Astrophys. 5, 4.

Walker, A. B. C., Jr., Rugge, H. R., and Weiss, Kay, 1974a, Astophys. J. 188, 423, (Paper I).

1974b, Coronal Abundances Derived from X-ray Observations II:Nitrogen, Oxygen, Neon, Magnesium, and Iron, to be published in the Astrophysical Journal (August 15) (Paper II).

Withbroe, G. L., 1971 in The Menzel Symposium on Solar Physics, Atomic Spectra, and Gaseous Nebulae, (Ed. K. B. Gebbie)NBS Special Publication 353 (U. S. Govt. Printing Office, Washington) p. 127.

FIGURE CAPTIONS

Fig. 1 Portion of the spectrum recorded by the KAP spectrometer on OV1-17 for 20 March 1969, showing the Fe XVII $2s^2 2p^6\ {}^1S - 2s2p^6 3p\ {}^1P$ and ${}^3P$ lines.

Fig. 2 Portion of the spectrum recorded by the KAP spectrometer on OV1-17 for 20 March 1969, showing the Fe XVII $2s^2 2p^6\ {}^1S - 2s^2 2p^5 3d\ {}^1P$, ${}^3D$, and ${}^3P$, and $2s^2 2p^6\ {}^1S_0 - 2s^2 2p^5 3s\ {}^1P_1$, ${}^3P_1$ and ${}^3P_2$ lines.

Fig. 3 Level diagram for Fe XVII, showing the principal decay paths for the first 36 excited levels. Those levels with transitions to the ground level are shown in bold type.

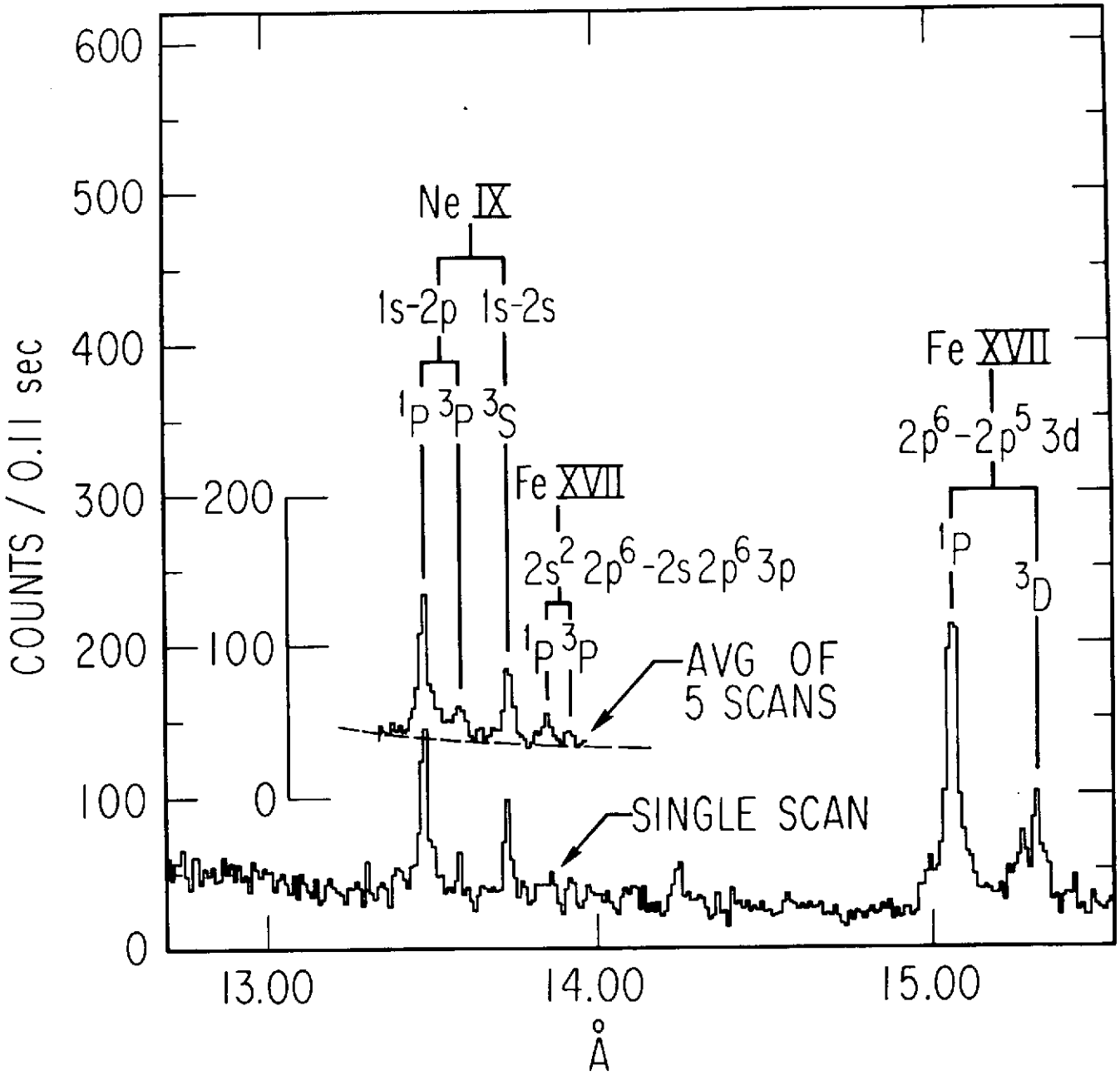
600
500
400
300
200
100
0
COUNTS / 0.11 sec
200
100
0
Ne IX
1s-2p 1s-2s
1P 3P 3S
Fe XVII
2s2 2p6-2s 2p6 3p
1P 3P
AVG OF
5 SCANS
SINGLE SCAN
Fe XVII
2p6-2p5 3d
1P
3D
13.00
14.00
15.00
Å

Figure 1

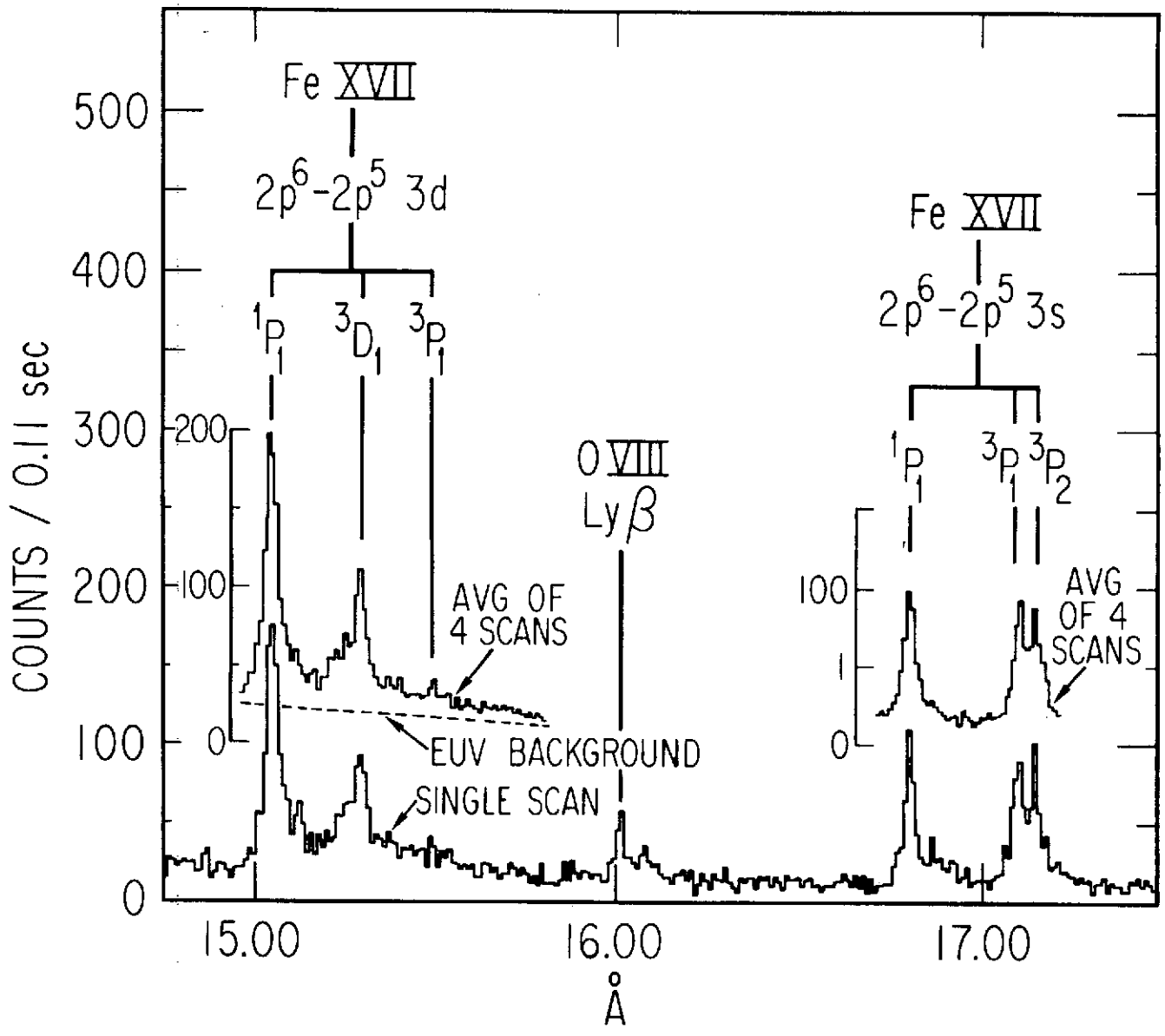
Fe XVII
2p6-2p5 3d
1P1
3D1
3P1
Fe XVII
2p6-2p5 3s
1P1
3P1
3P2
O VIII
Lyβ
AVG OF
4 SCANS
EUV BACKGROUND
SINGLE SCAN
AVG
OF 4
SCANS
COUNTS / 0.11 sec
500
400
300
200
100
0
200
100
0
100
1
0
15.00
16.00
17.00
Å

Figure 2

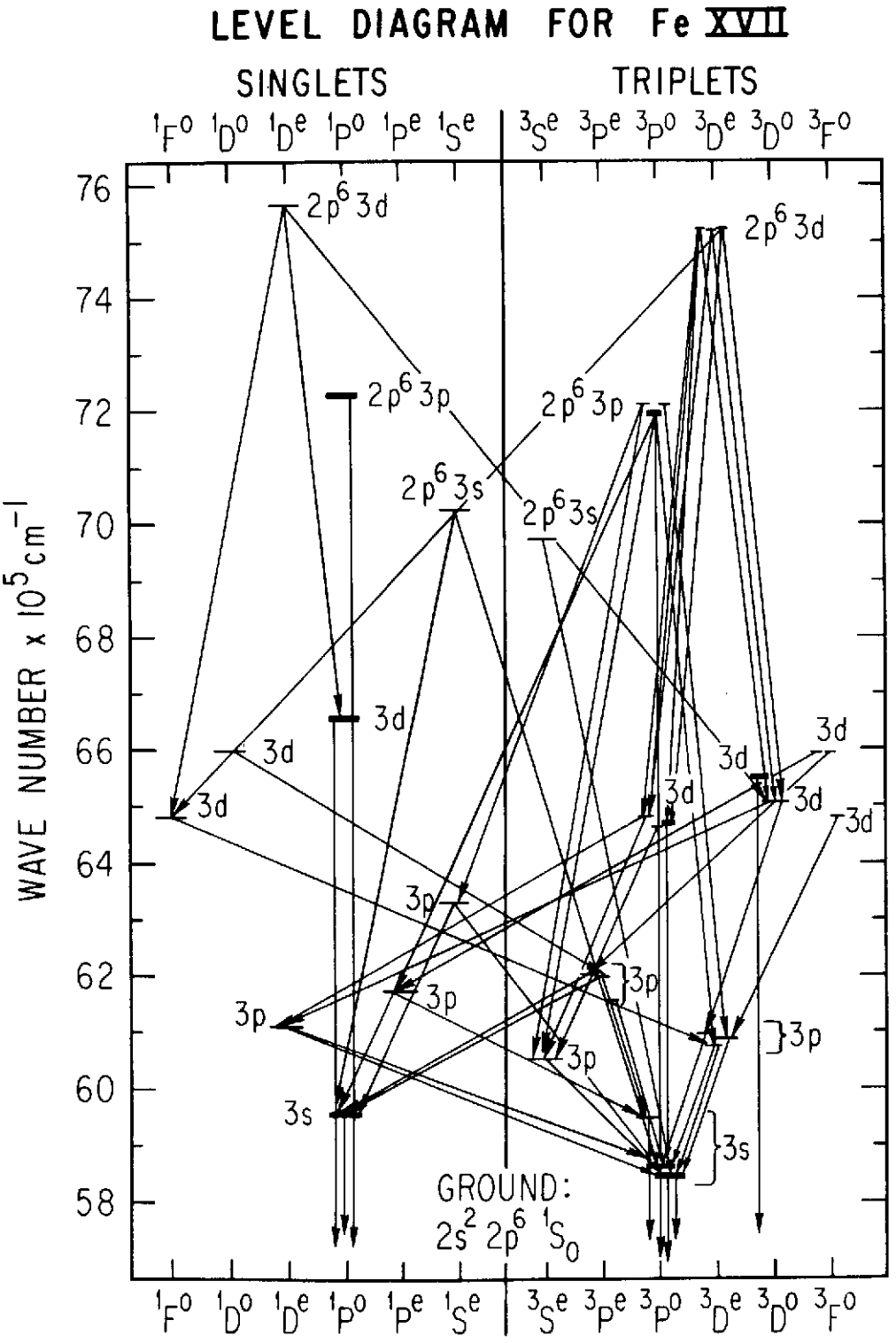
LEVEL DIAGRAM FOR Fe XVII
SINGLETS
TRIPLETS
$^1F^o$ $^1D^o$ $^1D^e$ $^1P^o$ $^1P^e$ $^1S^e$
$^3S^e$ $^3P^e$ $^3P^o$ $^3D^e$ $^3D^o$ $^3F^o$
WAVE NUMBER x 10^5 cm^{-1}
76
74
72
70
68
66
64
62
60
58
$2p^6\,3d$
$2p^6\,3p$
$2p^6\,3s$
3d
3p
3s
GROUND:
$2s^2\,2p^6\,^1S_0$

Figure 3